Evaluation of Fatigue Life and Retrofitting on the Benicia-Martinez Bridge

JOHN M. HANSON, MICHAEL J. KOOB, AND JOHN W. FISHER

An evaluation of the fatigue life of the Benicia-Martinez Bridge was undertaken in anticipation of the widening of the bridge. This 1.2 mile long, high level crossing includes ten steel deck-truss spans up to 528 ft in length. Welded built-up H sections of T-1 and ASTM A242 steel were used for the truss members. Stay plates were also fillet welded to the flanges of the H-sections at the joints, apparently to offset the loss of section due to bolt holes.

Cracking had been found at several fillet weld terminations of the stay plates prior to the evaluation. Subsequent examination during the course of the evaluation confirmed that fatigue crack growth had occurred, even though most of the previously-observed cracking was related to fabrication.

A state-of-the-art evaluation of the fatigue life was made using strain data recorded under normal traffic. This evaluation revealed that, on a conservative basis, the fatigue life was nearly exhausted. Details to remove the fatigue-sensitive conditions were developed and subsequently implemented.

INTRODUCTION

The Benicia-Martinez Bridge, located thirty miles northeast of San Francisco, carries Interstate Highway 680 across the Sacramento River. This 1.2 mile long, high-level crossing consists of ten steel deck-truss spans ranging in length between 330 ft and 528 ft and eight steel plate-girder approach spans. A photograph of the bridge, looking south, is presented in (Figure 1).

The bridge was designed by the California Department of Transportation (CalTrans) in the late 1950s and has been in continuous service since it was opened to traffic in 1963. The design was based on AASHO and CalTrans specifications in effect at that time, using welded built-up steel H-sections for the truss members and bolted connections. The H-sections were fabricated using both T-1 and ASTM designation A242 plates. The T-1 plates conform to the current ASTM A514 specification. Stay plates were welded to the flanges of the H-sections at the joints in the truss members, apparently to offset the loss of section due to the bolt holes. A photograph of one of these locations is shown in (Figure 2).

An evaluation of the fatigue life of the main truss members of the bridge was undertaken in preparation for widening of the roadway. The evaluation was to have been based mainly on strain data and traffic records made by CalTrans. However, fatigue cracks were found at the ends of and along the fillet welds connecting the stay plates to the flange tips of the chord members. It was evident that retrofitting of this condition was desirable. Procedures for this retrofitting were developed and implemented which would allow the widening to proceed as planned. This paper describes the work carried out for this evaluation.

REVIEW AND INITIAL INSPECTION

The structural system consists of two parallel trusses joined by top and bottom plane lateral bracing and diagonal sway bracing. An elevation of a typical suspended and continuous span is shown in (Figure 3), and a typical cross-section in (Figure 4).

The so-called continuous span trusses are simply supported on the piers, and have 99-ft end cantilevers extending into the adjacent spans. The suspended span trusses are simply supported on the end cantilevers of the adjacent continuous span trusses. Dummy members are used at the ends of the suspended trusses. Each of the parallel truss systems is statically determinate.

Typically, the H-shaped sections were fabricated by fillet welding a web plate to two flange plates. The web and flange plates contain transverse groove welds, where there may be either a change in thickness or a change in the grade of steel. Top and bottom chord members are continuous between the five-member joints (i.e., continuous through the T-joints). The truss members are connected at the joints by gusset plates bolted to the flanges of the members. Additional "stay plates" were fillet welded to the tips of the flanges in the joint regions.

Mill reports for the 1-in.-thick flange plates indicated that five heats of steel had an ultimate tensile strength exceeding the limit of 130 ksi for A514 steel. The highest reported strength was 134.6 ksi. The yield strengths of these five heats ranged from 120.8 ksi to 125.3 ksi. The location in the bridge of steel plates from these heats, as well as mill information on plates thicker than 1 in., was not available. According to CalTrans, all groove welds were radiographed to assure that standards then in effect were met.

In accord with the current AASHTO specifications (1)*, the fillet welds connecting the web plate to the flange plates and the groove welds in the flange plates are Category B conditions. The fillet welds connecting the stay plates to the tips of the flange plates are also Category B along their length, becoming a condition between Category E or E' at their terminations. For this fatigue evaluation, it is reasonable to consider the detail to be a Category E' condition.

Since there are only two main trusses in the superstructure, the bridge is classified as nonredundant. Furthermore, in accord with the Guide Specifications for Fracture Control of Nonredundant Steel Bridge Members (2), the tension members in these trusses are fracture critical members, because their failure could result in collapse of the bridge.

The concrete roadway is supported on stringers which frame into transverse beams that are supported on the top

* Numbers in parentheses refer to references listed at the end.

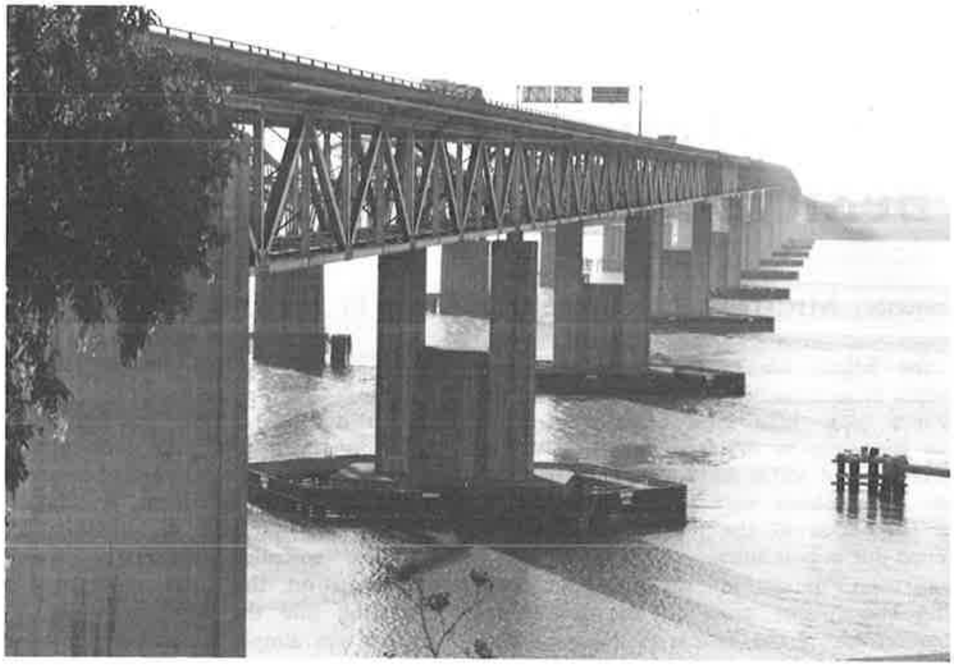

FIGURE 1 View of west side of bridge.

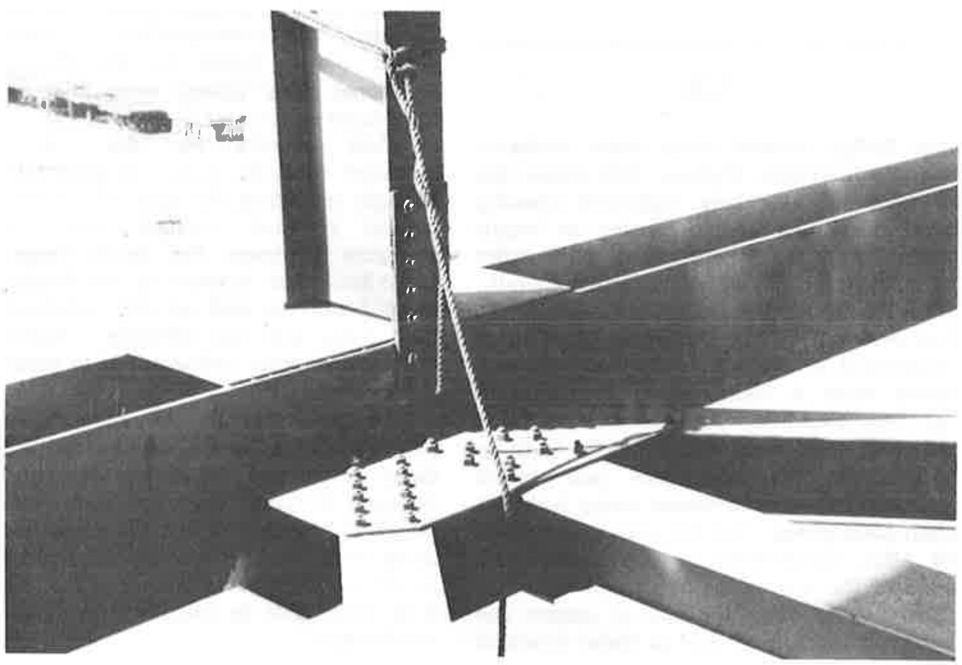

FIGURE 2 Stay plate welded to flange, at a T-joint.

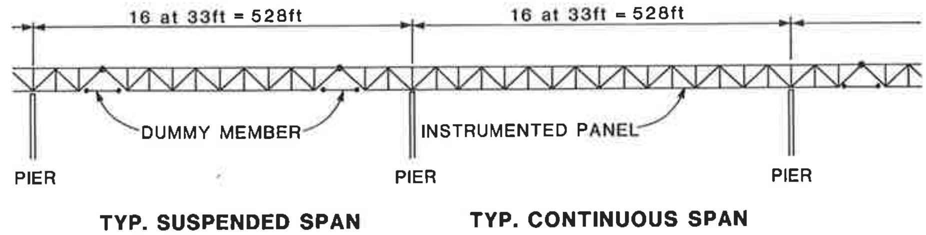

FIGURE 3 Continuous and suspended spans.

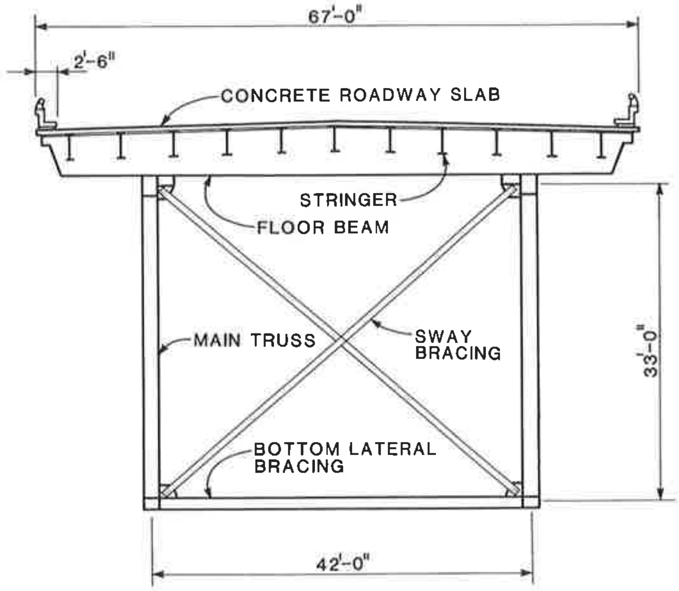

FIGURE 4 Typical cross section.

chord joints of the trusses. The evaluation of fatigue life did not include the welded connections in these members.

Structural analyses were performed by CalTrans based on two-dimensional and three-dimensional models of the bridge. The analyses showed that, under a moving truck load, members located at the approximate point of bending moment inflection under dead load in each continuous span are subject to the highest stress range. These members are subject to relatively small axial forces under dead load and are therefore of relatively small cross-sectional area. Under a moving truck load, however, they are subject to a significant axial force range.

An initial inspection of the bridge was made to gain first-hand familiarity with the fatigue-critical conditions. The quality of the welding was observed to vary from span to span. The fillet welds connecting the stay plates to the edges of the flanges were particularly uneven with indications of discontinuities, possibly because they were made in the field and also because some of the welds were made in the overhead position. The geometry of the wrap-around welds at the termination of the fillet welds varied considerably in shape, frequently appearing to be susceptible to cracking. Information provided by CalTrans indicated that cracks had previously been found at five locations. However, the nature of these cracks was not indicative of fatigue.

Several locations were observed where it appeared that there was overlapping in the fillet welds connecting the web plate to the flange plates, or where repairs had been made. At these locations, the weld profile was such that the fatigue strength might approach a Category E condition.

The roadway was to be widened from 62 ft-0 in. to 74 ft-0 in. by extending the transverse floor beams and the concrete deck slab. According to a three dimensional stress analysis made by CalTrans, when a single truck is located over one truss, 40 percent of the load is distributed by the bracing to the other truss. On this basis, stress due to a single truck will increase by approximately 5 percent after the widening is completed. As subsequently discussed, a stress range increase of this magnitude was recognized in the evaluation of fatigue life.

COLLECTION OF STRAIN HISTORY AND TRAFFIC DATA

From May 14, 1987 through June 3, 1987, strain data under general traffic loading were recorded by CalTrans on truss members in Span 5, a 528 ft span of the bridge. Data were recorded simultaneously from each gage for approximately 325 hours. During the collection of the strain data, the number of northbound vehicles crossing the bridge per day was recorded by CalTrans for each of several vehicle weight classes.

Strains were also recorded by CalTrans for four separate round trips of a permit vehicle crossing the bridge, in the absence of all but a few other relatively small vehicles. These strain data were recorded in the early morning of June 27, 1987. The permit truck was a 9-axle tractor-trailer weighing 204,000 lb. travelling at a speed of approximately 20 mph.

Locations of Instrumentation

Strain gages were installed at six locations in the top chord (U12-U13) and bottom chord (L12-L13) in the fifth panel from the north end of both trusses in Span 5. The locations of these 24 gages are shown schematically in (Figure 5).

Gages 3, 4, 9, and 10 in the west truss and gages 15, 16, 21, and 22 in the east truss were located at the mid-lengths of the chords and at the mid-widths of the flanges. Strains measured at these locations should not be influenced by bending moment or local strain concentration. Gages 5, 6, 7, and 8 in the west truss and gages 17, 18, 19, and 20 in the east truss were located on the flange tips, approximately one inch from the ends of the stay plates. At these locations the strains may be affected by both bending due to restraint of end-rotations and strain concentration at the ends of the stay plates. The gusset plates at the T-joint are relatively small and do not extend to the locations of the strain gages along the member. Gages 1, 2, 11, and 12 in the west truss and gages 13, 14, 23, and 24 in the east truss are located near the ends of the members and at the tips of the flanges, approximately one inch from the ends of the stay plates. However, they are also located slightly inside the edge of the gusset plates. Consequently, the strain at these locations may be reduced due to transfer of force in the member to the gusset plates, and may be affected by moment and strain concentration.

Traffic Records

During the recording of the strain data under general traffic loading, records were kept at the toll booths of the volume of northbound bridge traffic. Total daily bridge traffic in both directions was estimated as double that in the northbound direction. This traffic was in the range of 35,000 to 42,000 vehicles on week days, and 31,000 to 37,000 vehicles on weekend days.

The daily records include the number of vehicles in each of several different weight classifications. The largest stress cycles are associated with either trucks or heavy trucks. Heavy trucks are those having five or more axles. About 2700 trucks crossed the bridge each week day. On weekend days, only about one quarter as many trucks crossed the bridge. Fifty five percent of the total truck traffic was in the heavy truck classification.

Interpretation of Strain Records for the Permit Vehicle

Records of strain under the permit vehicle loading showed that the strain along the length of the instrumented tension chords had different amplitudes but nearly identical variations over time (time signatures), regardless of whether the permit vehicle was traveling northbound or southbound. For twelve of the gages, the maximum stress

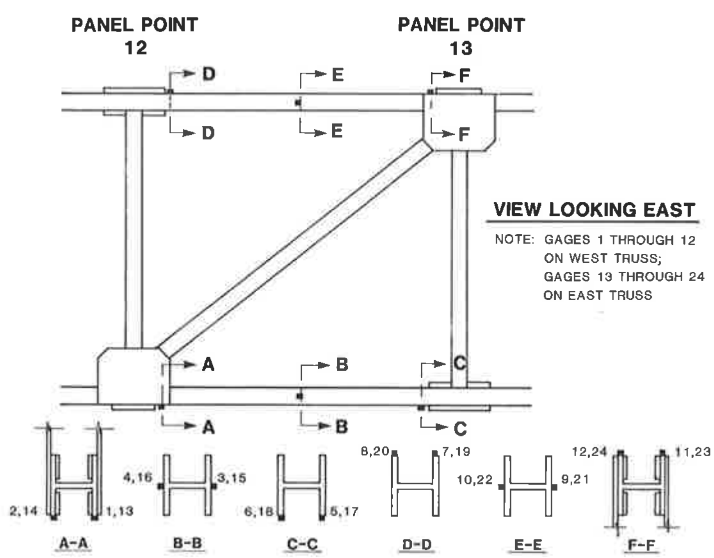

FIGURE 5 Stress gage locations.

ranges were computed. These ranges are given in Table 1. The reasonable agreement of the stress range for pairs of gages at a particular section indicates that the effect of out-of-plane and torsional distortions in these members under a heavy loading is small compared to the primary effect.

A simple pin-jointed truss analysis predicts that strain under load is constant over the length and width of a member. Table 1 shows that the recorded strains and derived stresses vary between the instrumented locations. The stresses are lowest at the gages near the five-member joints, and highest at the gages at the T-joints.

Several factors apparently interact and contribute to the variation of stress between the different gage locations:

1. Influence of strain concentration near the ends of the stay plate welds, which cause an increase in the stresses at these locations.
2. Bending at the ends of the members, which causes either an increase or decrease in the stresses at the tips of the flanges.
3. Overlapping of the gusset plates with the gages at the five-member joints.
4. Torsional deformation due to the location of the permit vehicle relative to the center of the bridge.

These factors are considered in the assessment of the stress range histograms.

DEVELOPMENT OF STRESS RANGE HISTOGRAMS

Stress range histograms were developed from the strain data using computer hardware and software especially developed for this purpose. The hardware consisted of a Compaq 386 desktop computer connected to peripheral devices. These devices included an EMI 7000C 28-channel tape recorder for reading the analog data from the tapes supplied by CalTrans, a DASH IV stripchart recorder for output of the strain records, and a Kyowa 116B Analog/Digital converter.

Previously written software for developing histograms from short segments of strain records was modified to allow continuous analyses of the strain records. The software performed a point-by-point analysis of the data from each channel, using a modified one-pass rainflow algorithm (3). In this algorithm, the cycle count in each stress range is accumulated as local maxima and minima are encountered in the strain data, and data that are not local maxima or minima are discarded. This algorithm does not retain the digitized data record.

The histograms were output in a form suitable for post processing with standard micro-computer software. Effective stress ranges and numbers of cycles for each strain data record were computed using Lotus 1-2-3(c) spreadsheet templates.

A total of 20 stress range intervals each 500 psi wide were used for the histograms, from zero to 10,000 psi. This selection was made on the basis of a visual examination of the recorded data and a desire for four to eight

TABLE 1 - MAXIMUM STRESS RANGES IN TENSION CHORD MEMBERS UNDER THE PERMIT VEHICLE LOADING

(a) Chord L12-L13 (West Truss)

		Channel					
Run	Direction	1	2	3	4	5	6
		Stress Ranges, in ksi					
1	Northbound	2.18	2.12	4.18	4.20	5.89	5.34
	Southbound	2.87	2.93	5.60	5.48	8.32	7.48
2	Northbound	2.58	2.55	4.96	4.84	6.84	6.26
	Southbound	3.25	3.31	6.32	6.24	9.37	8.41
3	Northbound	3.07	2.99	5.57	5.54	7.74	7.16
	Southbound	3.07	3.10	6.03	5.95	8.96	8.03
4	Northbound	2.55	2.49	4.76	4.61	6.50	5.92
	Southbound	2.99	2.99	5.54	5.74	8.56	7.74

(b) Chord L12-L13 (East Truss)

		Channel					
Run	Direction	13	14	15	16	17	18
		Stress Ranges, in ksi					
1	Northbound	2.55	2.64	4.47	4.47	6.93	6.47
	Southbound	2.70	2.50	4.29	4.32	6.12	5.77
2	Northbound	3.25	3.05	5.39	5.39	8.29	7.60
	Southbound	3.22	3.07	5.25	5.16	7.40	6.84
3	Northbound	3.63	3.48	5.96	6.06	9.31	8.47
	Southbound	2.90	2.73	4.70	4.76	6.67	5.86
4	Northbound	3.13	3.10	5.34	5.37	8.27	7.48
	Southbound	2.78	2.58	4.47	4.52	6.35	5.86

intervals containing a significant number of cycles. The data tapes were read on the EMI 7000C tape recorder at a tape speed of 15/16 inches per second, which helped to minimize noise contamination. A digitizing rate of 100 Hz provided adequate detail of the higher frequency components of the data, and allowed the computer to process the data in real time.

Sixteen of the 24 data channels on each tape were selected for processing. The selected channels are noted with asterisks in (Figure 5). All six data channels in each bottom (tension) chord member were processed, since these members are subject to fatigue crack growth. The remaining four channels were selected in the top (compression) chord members, consisting of one mid-length gage (gage 10) in the west truss and one gage at each of the three member cross sections (gages 19, 22, and 23) in the east truss.

Production of Stress Range Histograms

During processing of the strain data tapes, measures were taken to detect and reduce possible noise contamination. An electronic air cleaner was used to remove dust. The heads of the tape recorder were cleaned before processing each tape to remove accumulated dust or tape residue. Also, processing was stopped a few minutes before the end of the data in order to avoid processing random noise after the end. Each histogram represented 297.7 hours of strain measurements. Data for selected histograms is given in Table 2. A histogram for channel 5 is shown in (Figure 6).

Effective Stress Range and Fatigue Cycles

For each of the 16 strain gages for which data were processed, the effective stress range and the number of equivalent stress cycles were determined from the stress range histograms. The effective stress range S_{re} was calculated using Miner's Rule (4):

$$S_{re} = [\sum_i \alpha_i S_{ri}^3]^{1/3} \tag{1}$$

where the summation is over all stress range intervals in the histogram, α_i is the fraction of the total number of stress range cycles that occurs within the i^{th} stress range interval, and S_{ri} is the average stress range for stress range interval i.

The corresponding number of equivalent stress cycles N_e was calculated from expression:

$$N_e = \sum_i N_i \tag{2}$$

where the summation is over all stress range intervals in the histogram, and N_i is the number of cycles counted for stress range interval i.

In both of the above summations, data for the lowest stress range interval (0 - 500 psi) and data above 10,000 psi were excluded. Stress ranges below 500 psi contribute very little to the effective stress range. Stress ranges above 10,000 psi were infrequent and did not have a significant effect on the effective stress range. Many appeared to be due to noise in the data from spurious signals.

The resulting equivalent stress ranges and numbers of cycles from these calculations are shown in Table 3 for each of the 16 strain gages for which data were processed.

Interpretation of Results

Several observations were made by studying the stress range histograms, the effective stress ranges, and the numbers of equivalent stress cycles for the different strain gage locations. First, both the effective stress range and the number of equivalent stress cycles vary over the length of the chord members. The variation in stress range is similar to that observed for the stress ranges under the permit vehicle loading. Second, both the effective stress range and the number of equivalent stress cycles vary appropriately with respect to location. This indicates that the data are reliable and relatively free of noise contamination. Third, both the effective stress range and the number of equivalent stress cycles are lower at the locations in the top (compression) chord members than they are in the bottom (tension) chord members. This probably is due to the larger cross sectional area and possibly some composite action of the top chord members with the deck. It should be recognized that fatigue crack growth is not critical when a member is in compression, because the growth will stop outside of any region of residual tension.

The variation in the effective stress ranges over the length of the chord members is consistent with the data recorded under the permit vehicle loading: the lowest stress ranges are at the five-member joints (Channels 1, 2, 13, and 14) and the highest stress ranges are next to the T-joint (Channels 5, 6, 17, and 18). Also, stress ranges from the gages at the mid-lengths of the chords (Channels 3, 4, 15 and 16) fall between those at the ends.

The number of equivalent stress cycles over the lengths of the members varies similarly. The relatively higher stress ranges from Channels 5, 6, 17, and 18 result in fewer cycles falling into the 0 to 500 psi stress range interval, which was neglected in the summations, resulting in a larger number of equivalent stress cycles for these channels. Just the opposite is true for Channels 1, 2, 13 and 14, resulting in a smaller number of equivalent stress cycles for these channels. For Channels 3, 4, 15 and 16, at the mid-length of a chord, the equivalent stress cycles fall between those for the two ends.

The variation in stress ranges and number of equivalent stress cycles over the lengths of the compression members follows the same trends discussed above for the tension members.

The procedure used for estimating the fatigue life of the welded connections is based on the nominal stress range, including axial force and moment components, but neglecting effects of strain concentration caused by the weld. None of the gage locations precisely meet these requirements. The gages near the mid-length of the chords are not influenced by bending, while the gages near the ends of the chords are influenced by strain concentration caused by the welds. Gages 5, 6, 17 and 18 best approximate the critical conditions. The strain concentration caused by the weld may slightly increase the effective stress range at these locations. On this basis, nominal values of S_{re} = 2.0 ksi and N_e = 71,000 were judged to best represent

TABLE 2 DATA FOR SELECTED STRESS RANGE HISTOGRAMS

Strain Gage No.			3	4	5	6	15	16	17	18
Bin Number	Stress Levels From: (ksi)	To: (ksi)								
0	0.00	0.50	4E+07	3E+07	4E+07	3E+07	4E+07	3E+07	4E+07	3E+07
1	0.50	1.00	20952	20284	41536	38001	21608	18830	42784	37396
2	1.00	1.50	7984	7828	10205	10218	7875	7561	9348	9126
3	1.50	2.00	5460	5491	5931	5822	5405	5234	5748	5595
4	2.00	2.50	4180	4034	4200	4274	3807	3597	4159	3961
5	2.50	3.00	1961	1768	3299	3414	1461	1140	2948	3034
6	3.00	3.50	534	494	2643	2638	424	357	2343	2511
7	3.50	4.00	238	227	2136	1435	171	138	2001	1329
8	4.00	4.50	82	77	1016	500	60	47	913	469
9	4.50	5.00	32	24	412	256	28	16	379	229
10	5.00	5.50	18	17	217	131	19	12	183	97
11	5.50	6.00	11	6	104	65	4	9	97	49
12	6.00	6.50	6	5	52	36	3	4	53	32
13	6.50	7.00	4	9	26	15	5	4	27	16
14	7.00	7.50	4	7	18	12	4	2	14	7
15	7.50	8.00	5	5	8	6	3	4	14	12
16	8.00	8.50	2	2	6	5	2	1	15	6
17	8.50	9.00	3	4	3	6	6	3	1	2
18	9.00	9.50	5	4	4	4	3	3	9	3
19	9.50	10.00	2	1	7	3	3	1	5	1
20	10.00	and over	30	13	44	74	13	10	62	39

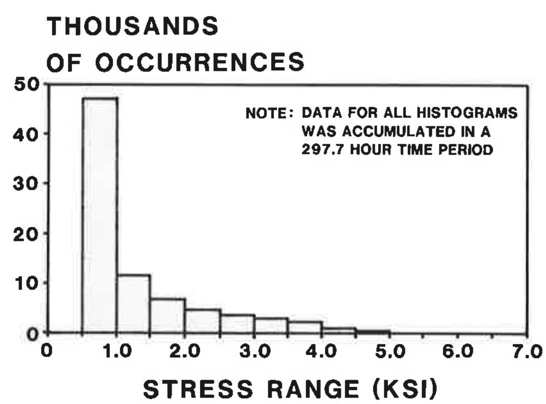

FIGURE 6 Stress range histograms for channel 5.

TABLE 3 EFFECTIVE STRESS RANGES AND NUMBERS OF CYCLES

Gage No.	Effective Stress Range, Ksi	No. of Cycles	Location
West Truss			
1	1.66	24909	behind gusset
2	1.35	23969	behind gusset
3	1.70	41483	mid-length
4	1.69	40287	mid-length
5	2.04	71823	at T-joint
6	1.93	66841	at T-joint
7	Not determined		
8	Not determined		
9	Not determined		
10	1.36	18291	mid-length of top chord
11	Not determined		
12	Not determined		
East Truss			
13	1.21	24945	behind gusset
14	1.25	23475	behind gusset
15	1.63	40891	mid-length
16	1.61	36963	mid-length
17	2.00	71041	at T-joint
18	1.90	63875	at T-joint
19	1.34	31910	top chord T-joint
20	Not determined		
21	Not determined		
22	1.56	27138	top chord mid-length
23	1.22	13770	top chord behind gusset
24	Not determined		

the critical stress range and corresponding number of cycles for the bridge. As discussed earlier, CalTrans' analysis indicates that live load stress ranges will increase by about 5 percent after the bridge is widened. Therefore, S_{re} = 2.1 ksi was used for the critical stress range in the widened condition.

ESTIMATION OF PAST AND FUTURE LIVE LOAD EFFECTS

In order to estimate past and future live load effects, it is assumed that the histogram and associated effective stress range represents a stationary process that does not vary over time, and that the cumulative number of equivalent fatigue cycles at any given gage location increases over time in linear proportion to the cumulative number of trucks estimated to have crossed the bridge since its opening in 1963.

Two measures of truck traffic were considered in the analysis. The first measure was the number of trucks with 5 or more axles, denoted as heavy trucks. The second measure was the total number of trucks, regardless of size, number of axles, or weight. This alternative measure could be more directly related than the first to the more frequent but lower amplitude stress ranges experienced by the bridge components.

The correlation between fatigue cycles and truck traffic volume was assessed by plotting the number of trucks that crossed the bridge during the time encompassed by each data tape against the number of equivalent fatigue cycles computed for the data tape. Although the number of fatigue cycles increased with increasing truck traffic, the data were widely scattered.

Based on these assumptions, past and future live load effects were incorporated into the fatigue life estimate using the following procedure:

1. An estimate was made of the total number of trucks that crossed the bridge while the strain data was collected. This number of trucks, denoted as T_{meas} was 51,860 for total truck traffic and 28,650 total heavy truck traffic.
2. Two-way average annual daily traffic (AADT) data for different vehicle classes was available for the years 1971 through 1985. An average of 6.2 percent of total vehicle traffic was trucks, and an average of 3.4 percent of total vehicle traffic was heavy trucks. These percentages were used to estimate total truck traffic and total heavy truck traffic from 1963 through 2010. This cumulative number of trucks was denoted as T_{TOT}.
3. For each strain gage, the cumulative number of fatigue cycles N_{TOT} experienced in each year was estimated from $N_{TOT} = N_e \times$ S.F. where N_e is the number of equivalent uniform amplitude fatigue cycles computed for the strain gage location (shown in Table 3) and S.F. is a scale factor relating the cumulative number of trucks having crossed the bridge by a given time to the number of trucks which crossed the bridge during the strain recording, expressed as S.F. = T_{TOT}/T_{meas}.
4. For each gage, two curves of the cumulative number of fatigue cycles N_{TOT} as a function of time were plotted, one in which only heavy truck traffic volumes are used for computation of T_{meas} and T_{TOT}, and the other in which all truck traffic volumes are used. The difference between the cumulative cycle curves provides an indication of the uncertainty in this aspect of the fatigue life estimate.

Using the procedure outlined above, the cumulative number of cycles vs time were tabulated. Plots of these results are shown in (Figure 7) for selected gage locations. It may be seen that the cycle curves developed from the total truck traffic are slightly higher than those based on heavy truck traffic. Therefore, cumulative cycles based on all-truck traffic were used to estimate fatigue life.

INSPECTION AND TESTING

The inspection was limited to Span 5 (east and west trusses) and Spans 9 through 12 (east truss) and, within these spans, primarily to horizontal chord members that are in tension. Attention was directed mainly to the fillet weld terminations at the ends of the stay plates, and to indications of discontinuities in the fillet welds along their length. The procedure generally included the following steps:

1. A visual examination was made for indications of cracking or discontinuities.
2. Where the examination revealed potential discontinuities, light grinding was performed to remove paint and clean up the weld toe.
3. After grinding, the surface was cleaned with a solvent.
4. Magnetic dry-particle testing was performed using an articulated-leg magnetic yoke and 110 volt, 60 Hz alternating current, in general accordance with ASTM E-709.
5. Where crack-like indications were found, light grinding was continued to verify that they extended into the base metal (i.e., the flange tip of the chord member). Some indications were removed in the grinding process.

A total of 242 stay plate welds at 35 connections were inspected. Ground areas were repainted. Cracks that extended into the base metal were found at four locations. The cracks occurred at either weld terminations or at a transverse discontinuity that was observed in the weld along the length of a stay plate.

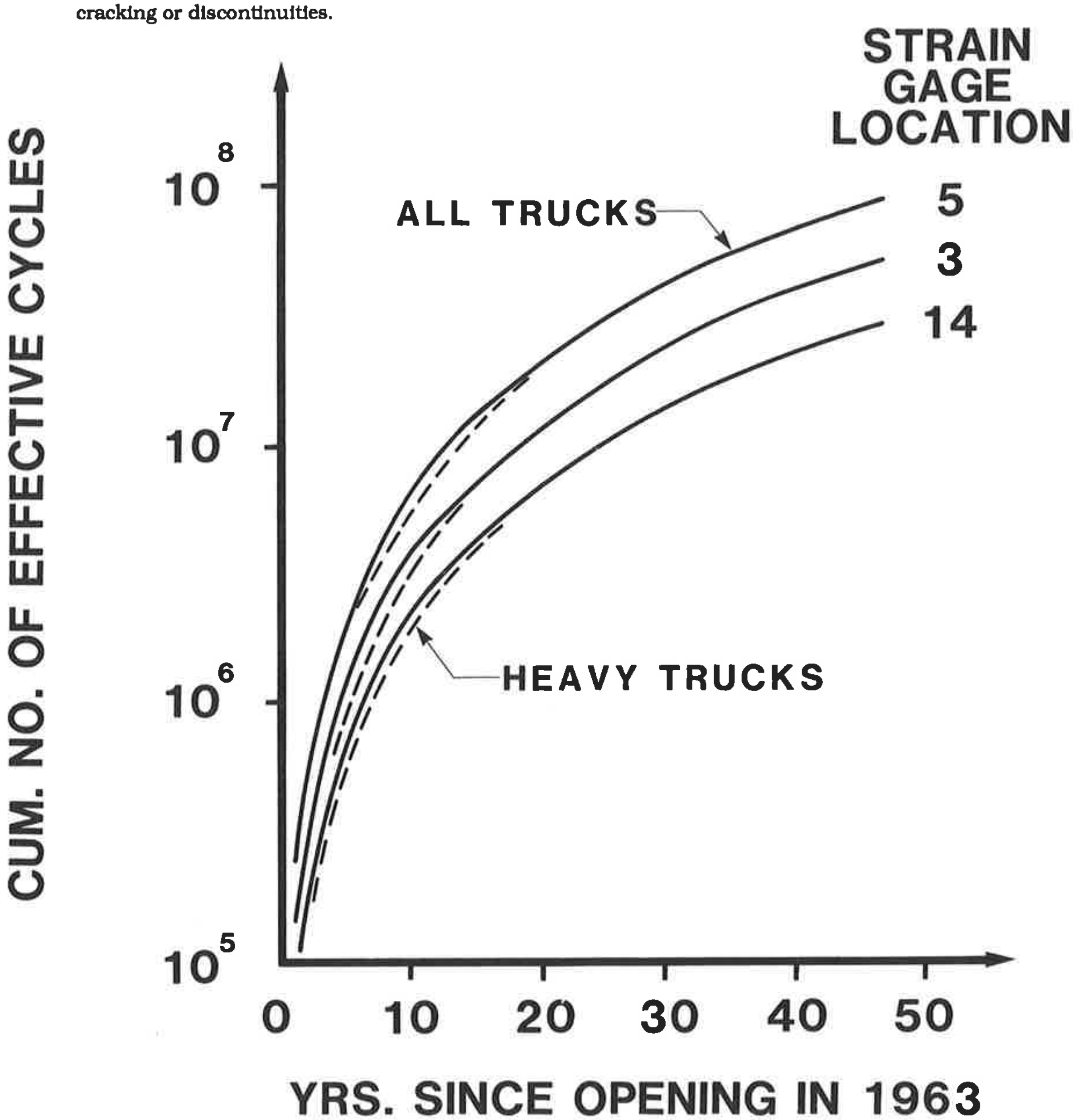

FIGURE 7 Cumulative cycle estimates.

Fractographic Examination of Cracks

All four indications of cracks or discontinuities were removed by coring. Metallographic and fractographic examinations indicated that fatigue crack growth had occurred at all four locations. Cracks at weld terminations had a length of about 3/8 inch. The examinations indicated that the crack growth rate was near the threshold level. The transverse crack through the fillet weld is believed to have started during fabrication as a hydrogen-related crack.

Additional cracks were also found emanating from the roots of the fillet welds, which appeared to have occurred during fabrication due to hydrogen. These cracks also appeared to have extended due to fatigue.

Tests on Cores Extracted from Bridge

A total of 20 cores were extracted by CalTrans. The core locations were selected to range over the entire length of the bridge, since steel heats would have varied within different regions of the bridge. They were also selected to be taken from flanges of compression members whose thicknesses best represented the range of flange thicknesses for the tension chord members. The cores had a diameter of 4 in.

All of the Charpy V-notch (CVN) tests were performed by CalTrans. The average of the three test results at each temperature level for each core are plotted in (Figure 8). It is apparent that the material from Core No. 8, which was from the east truss of Span 11, had a lower fracture toughness than material at the other locations. This is the only result that did not meet the minimum AASHTO requirement (1) of 35 ft-lbs at 0 deg F for A514 steel in a Zone 1 or Zone 2 service application.

The compact tension tests were made by Materials Research Laboratory, Inc. of Glenwood, Illinois. They were performed at 0 deg F in accordance with ASTM E399-83, except that the loading rate was approximately one second to failure. This loading rate is more representative of the conditions associated with bridge loadings than the dynamic rate given in E399. The cores were machined to obtain a test specimen with W equal to 3 in. The thickness of specimens from Core Nos. 7B and 8A was 1.5 in. The thickness of the other cores was reduced by machining only enough to clean the surface.

Results of the tests are given in Table 4. All test results were invalid according to ASTM E399 criteria, as anticipated, because the thickness of the flanges from which the cores were extracted was less than required by the test method, and also because the toughness of the material was higher than for brittle materials for which the test method was intended. However, the values of K_Q are considered to be a conservative estimate of K_{Ic}. The average of the four test values is 103 ksi sq root in.

An estimate of K_{Ic} was also made from the result of of the CVN tests, using the following upper-shelf correlation equation from Barsom and Rolf (5):

$$(K_{Ic}/\sigma_{ys})^2 = 5\,[(CVN/\sigma_{ys}) - 0.05] \qquad (5)$$

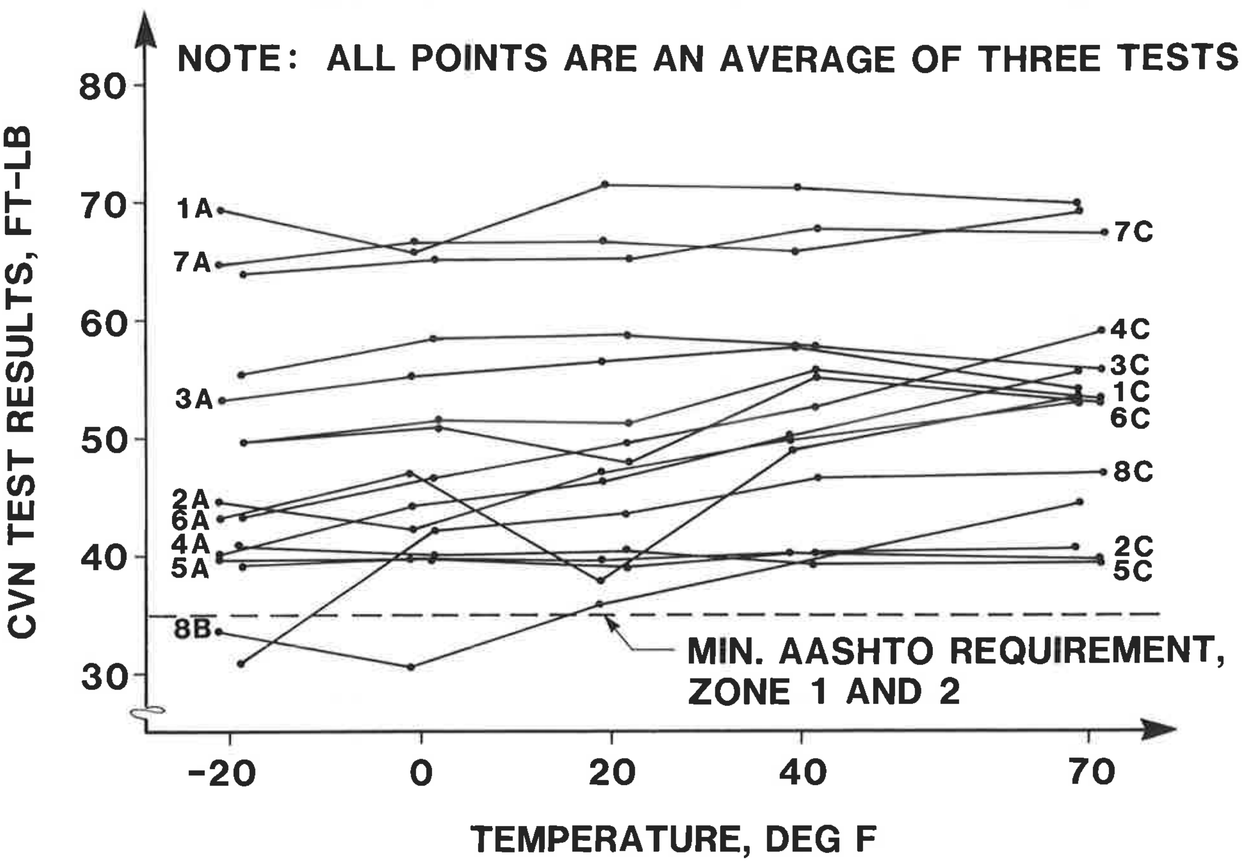

FIGURE 8 Charpy V-notch test results on cores of A514 steel.

TABLE 4 COMPACT TENSION TEST RESULTS

By MRL			By Fisher	
Core No.	K_Q (a) ksi$\sqrt{in.}$	R_{sd}	J Integral in. kip/in.^{2}	K_J (b) ksi$\sqrt{in.}$
1B	99.1	1.87	3.393	319
3B	102.2	1.85	2.290	262
7B	111.6	2.02	2.483	273
8A	100.8	1.72	2.020	246
Average	103.4	1.87	2.546	275

NOTES: (a) K_Q was computed as if there was no plastic yielding.
(b) $K_J = (EJ)^{1/2}$

Assuming that the yield strength, σ_{ys}, is equal to 100 ksi and the CVN is equal to 30 ft-lbs, the minimum value obtained in the test program at 0 deg F, K_{Ic} is equal to 112 ksi sq root in. Taking σ_{ys} equal to 125 ksi, the highest value from the mill test reports, K_{Ic} is equal to 122 ksi sq root in. These values are comparable with the value of K_Q equal to 103 ksi sq root in. obtained from the test program.

It was concluded that K_{Ic} equal to 150 ksi sq root in. was reasonable for an evaluation of the fracture resistance of the bridge. However, in view of the uncertainties with respect to the steel properties, the possibility for K_{Ic} as low as 100 ksi sq root in. was considered.

EVALUATION OF REMAINING FATIGUE LIFE

The estimate of the remaining fatigue life of the bridge was based on the following assumptions:

1. Through 1988, the time of this evaluation, the critical condition has been a Category E' detail at the termination of the fillet welds connecting the stay plates to the flange tips. This condition has been subject to an effective stress range of 2.0 ksi.
2. From 1989 on, the effective stress range should be increased to 2.1 ksi, to reflect the as-widened condition.
3. The cumulative number of effective cycles at any time under recorded and projected traffic is proportional to the total number of trucks crossing the bridge. The critical Category E' detail had accumulated 29,386,500 cycles through 1988, corresponding to 21,450,000 trucks crossing the bridge.

S-N curves, which relate the stress range S to the number of cycles N which can be resisted, have been established by AASHTO (1). However, recent tests and a review of all available data have led to new S-N curves published in NCHRP Report 286 (6). These curves were used for this evaluation. They are nearly the same as the AASHTO curves, and they were derived to expect with 95 percent confidence that 95 percent of the data would survive.

In NCHRP 286, S-N curves are given for both redundant and nonredundant load path structures. The curves for redundant structures are based on test data, while the ordinates of the curves for nonredundant structures are reduced by approximately 20 percent for additional conservativeness. The trusses in the Benicia-Martinez bridge are nonredundant. However, since an evaluation of the fatigue life is desired, the S-N curves derived directly from the test data were used. These curves are shown in (Figure 9).

In evaluating the fatigue life of the weld termination at the ends of the stay plates, the fatigue life cutoff given in NCHRP 286 was not used, because the existence of a fatigue limit below which no fatigue crack propagation occurs is considered to be assured only if all of the stress range cycles do not exceed the constant amplitude fatigue limit. This is not the case for the histograms developed in this analysis. The fractographic examination also showed that crack growth was occurring because some stress ranges were exceeding the crack growth threshold.

The NCHRP 286 S-N curves are compared directly in (Figure 9) to the assumed effective strength of 2.0 ksi and the accumulated number of equivalent stress cycles of 29,386,500 for the critical Category E' detail. It is apparent that the intersection of the two lines representing these conditions is close to the curve for the Category E' condition.

Two sources of uncertainty were recognized. The first is the uncertainty in the cumulative cycles, which is due mainly to the extrapolation of the data collected over a limited time interval to incorporate past and future life load effects over several decades. This uncertainty was accounted for by arbitrarily providing a $\pm$25 percent band around the cumulative truck traffic curve which was used for the evaluation. The second source of uncertainty is in the assignment of a fatigue category to the stay plate weld terminations. As pointed out earlier, the condition is believed to be between Category E and E', but was taken as Category E' to be conservative.

It may be seen from (Figure 9) that there is very little uncertainty associated with the predicted higher stress range of 2.1 ksi in the widened bridge. The narrow cross-hatched region represents the effective stress range before and after widening. The effect of the widening should be within the band, provided that the widening does not change the dynamic response of the bridge in a manner that would cause an amplification in the predicted stress range.

An iterative procedure was used to estimate the year in which the number of cycles and the combined stress ranges reaches the fatigue life corresponding to a Category E or E' condition. On this basis, the fatigue life is reached in 1995 for the Category E' condition, as illustrated in (Figure 10). Similarly for the Category E condition, the fatigue life is reached in 2018. Taking into account the

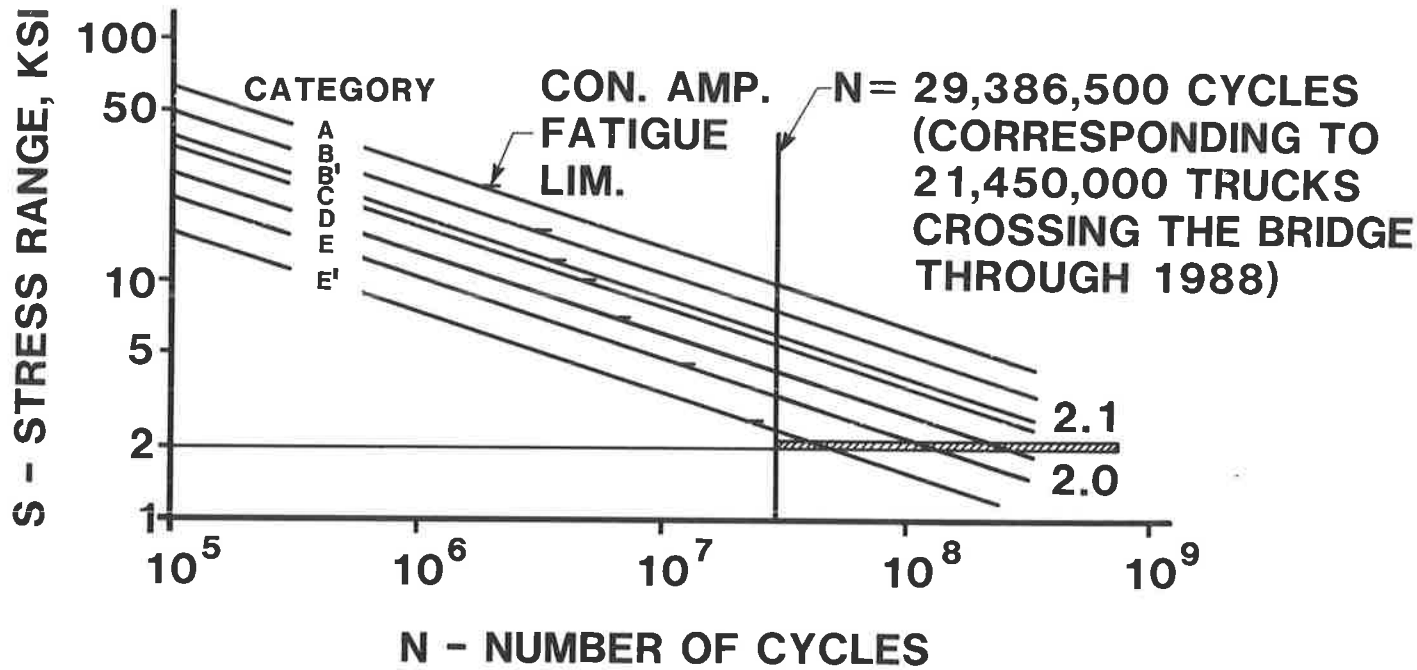

FIGURE 9 Estimated cycles compared to NCHRP 286 S-N curves.

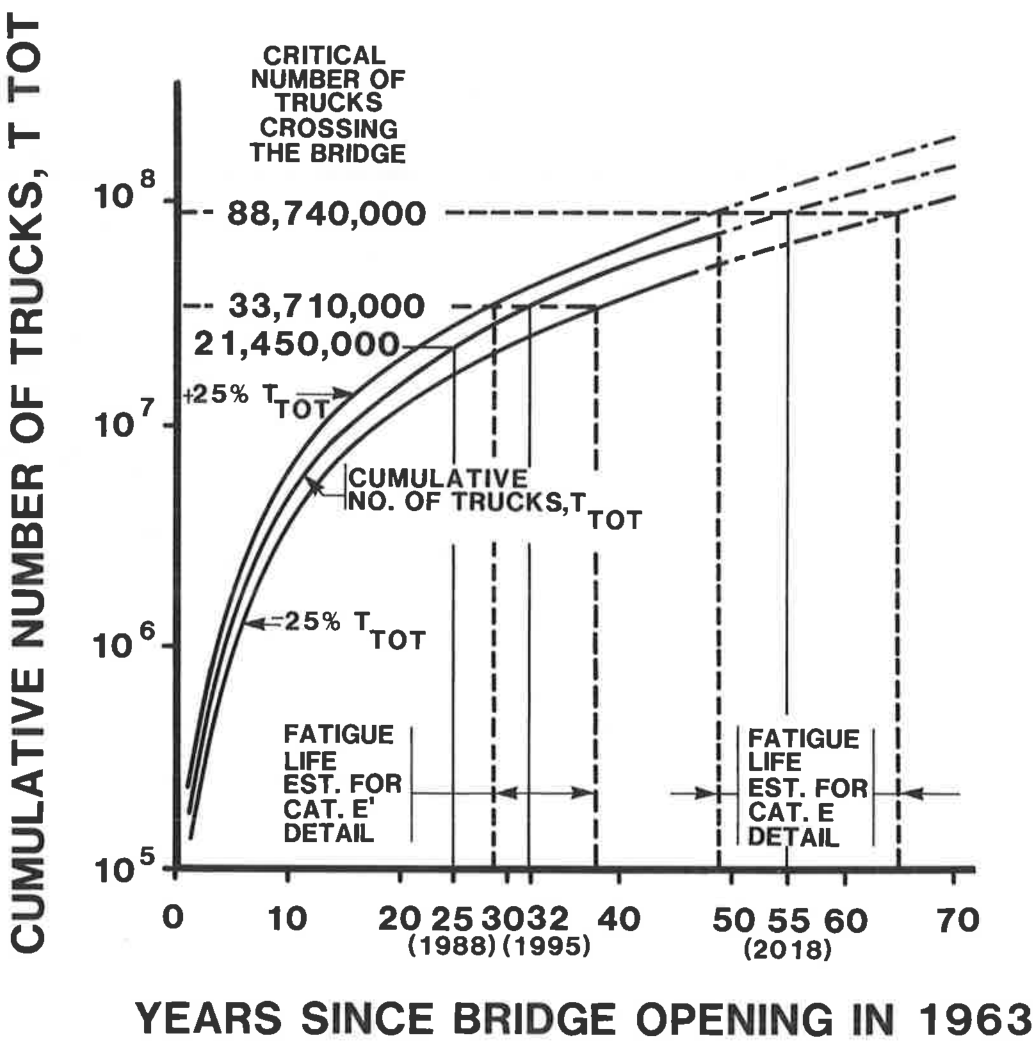

FIGURE 10 Fatigue life estimates.

uncertainty in the cumulative cycles, the estimated fatigue life for a Category E' condition is approximately 28 to 37 years, which corresponds to calendar years 1991 to 2000. In other words, taking a conservative position, the fatigue life of the bridge condition could be regarded as nearly exhausted. For a Category E instead of E' detail, the estimated fatigue life is much longer. The fatigue life for this case falls past the end of the traffic projections in 2010, but the fatigue life range could be extrapolated as 49 to 65 years, corresponding to calendar years 2012 to 2028.

Discussion

It is important to recognize that the state-of-the-art does not lead to a precise evaluation of fatigue life. There is uncertainty in the selection of the category for the wrap-around, fillet weld terminations on the stay plates. There is also uncertainty in the traffic estimates, in the correlation of the number of cycles associated with the effective stress range with the traffic estimate, and in the determination of the effective stress range.

It should also be recognized that the S-N curves on which the evaluation is based are lower bound estimates and represent a 95 percent level of probability that 95 percent of the conditions would achieve longer fatigue lives. Failure in a fatigue test is loss of load carrying capacity. Failure in a bridge may be fracture. Therefore consideration must also be given to the critical crack sizes that may cause a fracture.

For the Category E' condition at the termination of the fillet welds on the stay plates, it will be assumed that a fatigue crack will grow as a shallow semi-elliptical crack across the flange tip, becoming an edge crack condition as the crack advances. The stress intensity factor for a semi-elliptical surface crack is given by (5):

$$K_I = 1.12\,\sigma\sqrt{\pi a/Q}\,M_K \qquad (3)$$

where

- K_I = stress intensity at the crack tip, ksi sq root in.
- σ = in situ stress close to the crack tip, ksi
- α = crack depth, in.
- Q = flaw-shape parameter
- M_K = correction factor, say 1.0

From (Figure 2.13) of Ref. 5, Q will be about 1.0 for the condition being considered. Then

$$K_I = 1.12\ \sigma\sqrt{\pi a} \qquad (4)$$

which is the equation for an edge crack condition.

The relationship between a and σ as expressed by Eq. (4) is plotted in (Figure 11) for K_I equal to 100 ksi sq root in. and 150 ksi sq root in. As discussed earlier, K_I equal to K_{Ic} of 100 ksi sq root in. is considered to be the worst possible condition. K_I equal to K_{Ic} of 150 ksi sq root in. is considered to be a more probable representation of the toughness of the steel.

Crack tips are often located in regions of high residual stress, in which case σ may be equal to the yield stress of the steel. The only information on yield strength came from the mill reports for 1-in.-thick steel plate. These yield strengths ranged from 108 to 125 ksi. As indicated in (Figure 11), a crack that is approximately 0.15 in. deep could induce a fracture (under a dynamic vehicular loading) if σ was 125 ksi and K_{Ic} was 100 ksi sq root in. However, it is more likely that the critical crack size will be of the order of 0.35 to 0.5 in. deep, corresponding to K_{Ic} equal to 150 ksi sq root in. Considering the small size of the fillet welds, even a 0.15-in.-deep crack is probably outside of the region of high residual stress. Taking σ equal to an assumed maximum in situ stress of say 40 ksi, it may be seen from (Figure 11) that the critical depth of crack should be at least approximately 1.5 in., and more likely about 3.5 in.

In view of the limited extent of the inspection of the fillet weld terminations, it would not be surprising if cracks that are 0.15 in. deep exist at some locations in the bridge. The crack growth threshold for the fillet weld terminations on the stay plate is about 2 ksi, and hence growth should be expected. While it is probable that a crack at these locations would need to grow to a depth of at least 1.5 in. to be critical, as noted in the previous paragraph, the view that the fatigue life could be close to exhausted is reasonable with respect to the observed conditions. Consequently, it is believed to be highly advisable to remove these potentially critical Category E' conditions from all of the fracture-critical members in the bridge, or to provide reinforcement across a potential crack location.

For the Category E condition corresponding to a transverse crack through a fillet weld along the edge of the stay plate, the fatigue crack will also grow as a semi-elliptical crack from the junction of the weld and the flange tip. Thus Eq. 3 should approximately represent the condition. However, at shallow depths, Q should be greater than one, because crack growth into the flange tip will initiate from the region of the weld. Hence K_I is reduced, and it seems likely that the crack would have to grow out of the region of high residual stress before becoming critical. At greater depths, the condition will be the same as that at the termination of the weld at the end of the stay plate.

Although crack growth from a transverse crack through a fillet weld along a stay plate should be less critical than for the weld terminations, the potential for a critical condition developing should be recognized. Therefore it was deemed advisable to provide reinforcement through the T-joints in order to provide an alternate load path in the event of a fracture. The gusset plates at the five member joints may provide an acceptable alternate load path, without through joint reinforcement. It was recommended that these welds should be ground and inspected in an effort to locate and remove the discontinuities, irrespective of whether the joints are reinforced.

For the fillet welds connecting the web plate to the flanges of the chord members, and for the groove welds in the flanges, the condition is more complex. Because of the larger size of these welds, any defect or crack must be regarded as being in a zone of high residual stress equal to the yield strength. Experience indicates that K_I for any internal crack growing from an embedded flaw should be penny-shaped, and therefore K_I can be approximated from (5):

$$K_I = 2\alpha\sqrt{a}\,/\,\sqrt{\pi} \qquad (5)$$

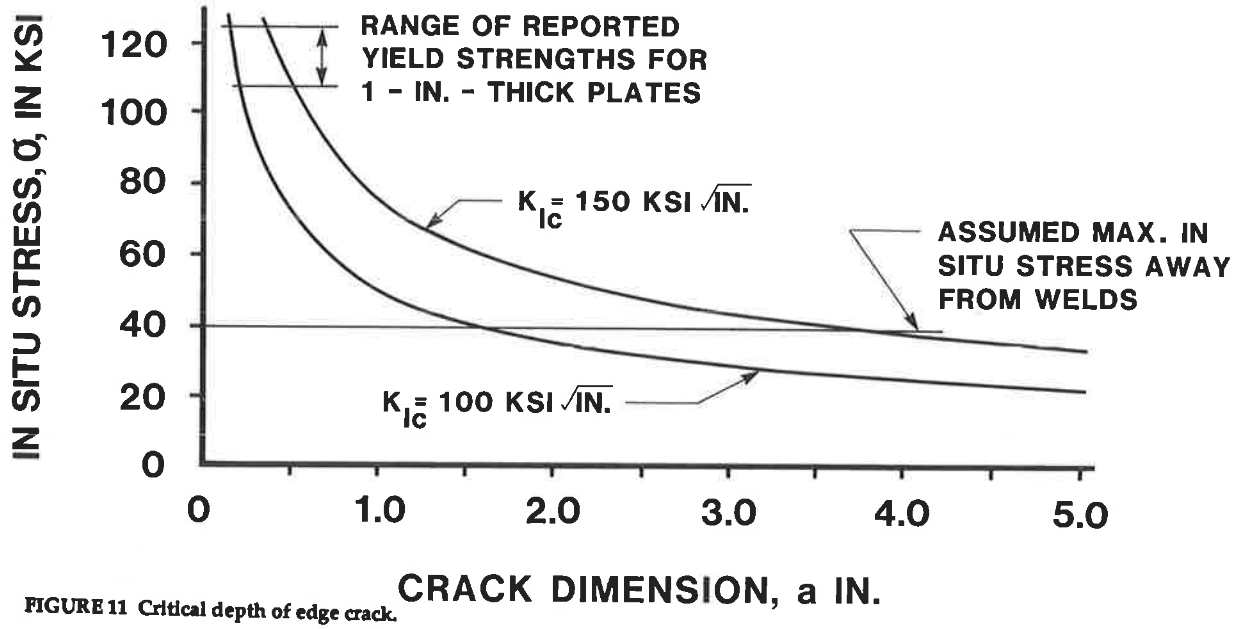

FIGURE 11 Critical depth of edge crack.

where a = the radius of a circular approximation of the internal crack.

Taking K_I equal 100 ksi sq root in. and σ equal to 125 ksi, a is equal to 0.5 in. Thus such an internal crack should have an overall size of about 1 in. and should also extend into base metal in order to have the potential for causing a brittle fracture. A crack growing from a surface defect should also reach the same overall size before becoming critical, because it will grow radially from the initiating defect.

In view of the lack of information about the fillet welds connecting the web plate to the flanges of the truss members and to the groove welds in the flanges, further examinations were deemed to be advisable. In particular, locations where there are irregularities in the fillet weld profiles or where repairs may have been made should receive close scrutiny by means of magnetic particle or dye penetrant inspection. Some percentage of the groove welds should be examined ultrasonically, and the results of this testing should be used to decide whether further examinations are needed. If an indication of crack growth is found, the region should be removed by coring and the indication should be exposed for fractographic examination.

CONCLUSIONS AND RECOMMENDATIONS

An evaluation of the remaining fatigue life of the Benicia-Martinez Bridge was made that indicates that the fatigue life should be regarded as close to being exhausted for the fillet weld terminations at the ends of the stay plates. In view of this finding, it was recommended that the fatigue-sensitive conditions associated with the stay plates located on the tension chord members be retrofitted, as subsequently discussed in this chapter.

It was also recommended that further examinations and testing be conducted on the groove welds in the flanges and on the fillet welds connecting the web plate with the flanges in the tension chord members. If indications of defects are found, samples of the defects should be extracted by coring for fractographic examination of the defects.

It was also recommended that a three-dimensional nonlinear analyses of the bridge be made in an effort to predict whether the loss of a tension member in a truss would lead to a collapse, or whether there are alternative load paths in the deck and bracing that could sustain the bridge.

Proposed Retrofitting

It is believed that the fatigue life of the bridge can be extended considerably by retrofitting the fatigue-critical conditions at the stay plates in fracture-critical tension chord members. Several retrofit measures are recommended, both to remove the critical Category E' conditions at the terminations of the fillet welds and to also add reinforcement that provides an alternate force path at all tension chord member T-joints. While the addition of reinforcement will reduce the stress range, the capability of that reinforcement to prevent a fracture will depend on the size of the initial defect and the accumulated fatigue damage. Thus the extension of fatigue life is uncertain, particularly for the defects along the fillet welds.

Core holes at stay plate weld terminations

The Category E' condition at the terminations of the fillet welds connecting the stay plates to the tension chord flanges are probably the most fatigue-critical details in the trusses. These details can be largely shielded from any stress range by drilling a partial core hole at these locations and then finishing the surface by grinding. The core holes should remove any existing cracks which may be subject to fatigue crack growth, but this should be verified by nondestructive examination. A detail of the recommended procedure is shown in (Figure 12).

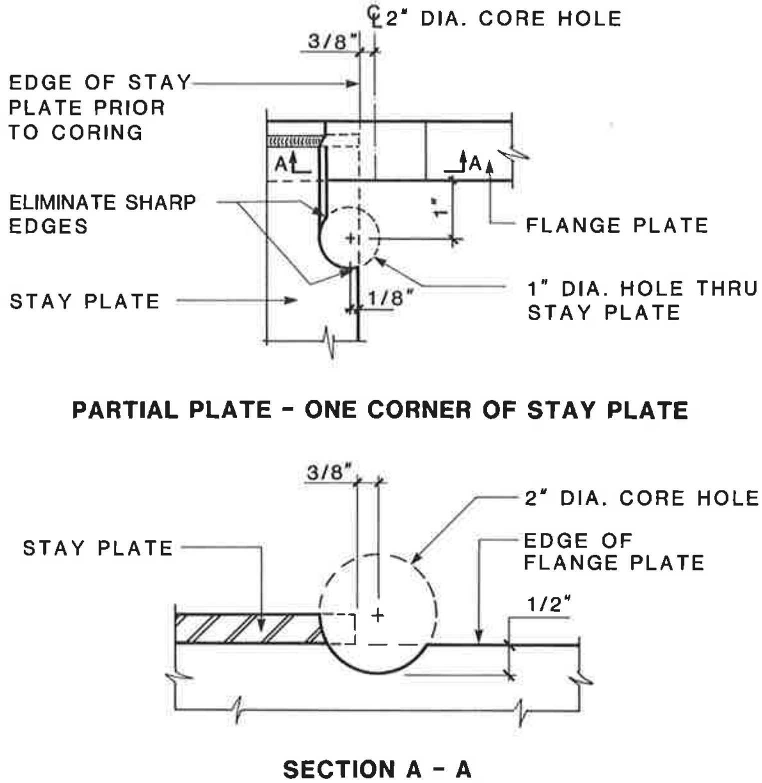

NOTES:

1. At locations of lateral gusset plate connections, a small portion of the lateral connection plate and some bolts from the vertical gussets will have to be removed in order to core through end of stay plate.
2. Grind cut surface of stay plate to remove any irregularities. Finish all ground surfaces to a surface roughness (R_A) of 500.
3. Clean exposed steel surface to remove any contaminants and paint.

FIGURE 12 Retrofitting detail for T-joints.

Strap plates at joints in tension

A discontinuity along the length of the stay plate fillet welds is a Category E condition, and is thus subject to fatigue crack extension. This condition cannot be shielded by coring. Therefore, an alternative redundant load path should be available in case of a fatigue failure initiated by such a discontinuity. Steel strap plates across the joints would provide an alternate load path. They would also reduce the subsequent stress range, reducing the likelihood of a fatigue failure. Strap plates should prevent a failure if a fracture occurs in the chord, but it still may be necessary to repair damage associated with the fracture. The accessible fillet welds should be ground in an effort to locate and remove the discontinuities, even though strap plates are installed.

At the five-member joints, the large gusset plates may possibly provide an acceptable alternate load path. It is recommended that a special analytical investigation of these joints be made in order to confirm that the load path provided by the gussets is acceptable. Otherwise these joints should also be reinforced.

At the T-joints, which have much smaller gusset plates, an alternate load path does not exist. At these locations, strap plates can be bolted to either the webs of the members or to the flanges. The strap plates must be effective beyond the ends of the stay plate welds in order to function as required.

Fatigue Life After Proposed Retrofitting

The fatigue life of the Benicia-Martinez Bridge will be extended substantially by the proposed retrofitting procedures. All of the Category E' details at the weld terminations at the ends of the stay plates on the tension chord members of the trusses should be eliminated.

The next most severe condition is the potential discontinuities in the fillet welds along the stay plates. These could be Category E conditions. Where they can be inspected, the discontinuities can be eliminated by grinding. Further, the fatigue life at the location of a discontinuity that cannot be eliminated may be increased because the stress range will be reduced by the strap plates or the gusset plates. While it appears that the increase should be substantial, the magnitude is difficult to assess.

The fatigue life of the fillet welds connecting the web to the flanges of the chord members and of the groove welds in the chords should be very high, and possibly without limit if the stress ranges are below the crack growth threshold. However, this expectation absolutely requires that there not be defects in these welds which will cause crack growth under cyclic loads.

Finally, it is important to keep in mind that the Benicia-Martinez Bridge is a very large structure. Unless the bridge can sustain without collapse the loss of a main load-carrying member in tension, even one undiscovered defect of critical size has the potential to cause a collapse. As previously discussed, further evaluation of this bridge is recommended, including additional material testing, inspection and nondestructive testing of the Category B conditions, and analysis of alternate load paths. Such evaluation will give greater assurance for the long range, safe use of the bridge.

IMPLEMENTATION OF THE RETROFITTING

The recommended retrofitting was subsequently included in the construction work for widening of the bridge. The prime contractor was Kiewit Pacific Company. With the approval of CalTrans, WJE undertook the coring work at the stay plate weld terminations as a subcontractor to Kiewit Pacific. This work was accomplished in the first half of 1989.

In total, about 1800 weld terminations were retrofitted. No effort was expended to examine the coring remnants for fatigue cracks, as this would have required further sectioning and testing. However, cracks extending from the root of the fillet welds were observed frequently.

Retrofitting of the stay plates was accomplished by coring a partial depth hole using a drilling template. This template was clamped to the flange. Magnetic base drill presses were used for the work.

The A514 material and weld metal used in the bridge was found to be very hard with poor machinability. Carbide tipped cutters were used. It was found that carbide tools cut approximately 10 times more holes than cutters made from high speed steel. Removing material by milling was also attempted on a trial basis. Again it was determined that high speed steel cutters did not perform in this material.

ACKNOWLEDGEMENTS

The authors wish to recognize and extend their appreciation to all of the people who assisted with and contributed to this evaluation. Personnel of CalTrans, including particularly Lee Everett, Bill Crozier, Richard White, Mark Seyed and Roger Caudle, were very helpful and supportive. Abolhassan Astaneh-Asl at the University of California at Berkeley and John O'Donnell at Materials Research Laboratory, Inc. provided valuable assistance. Other WJE staff that contributed substantially to the project included Stuart Werner, Dirk Heidbrink, Conrad Paulson, Roger Pelletier and Victor Monroy.

REFERENCES

1. American Association of State Highway and Transportation Officials (AASHTO). *Standard Specifications for Highway Bridges, Thirteenth Edition 1983 as Amendment by Interim Specifications - Bridges*, Washington, D.C., 1984, 1985 and 1986.
2. American Association of State Highway and Transportation Officials (AASHTO). *Guide Specifications for Fracture Control of Nonredundant Steel Bridge Members*, Washington, D.C., September 1978, updated 1986.
3. Downing, S. J. and Socie, D. F. Simple Rainflow Counting Algorithms. *Int. J. Fatigue*, January 1982.
4. Brockenbrough, R. L. and Johnston, B. G. *USS Steel Design Manual.* Pittsburgh: United States Steel Corporation, 1981.
5. Barsom, J. M. and Rolfe, S. T. *Fracture and Fatigue Control in Structures*. Second Edition, 1987.
6. Keating, P. B. and Fisher, J. W. Evaluation of Fatigue Tests and Design Criteria on Welded Details. *National Cooperative Highway Research Program (NCHRP) Report 286*, Washington, D. C. Transportation Research Board of National Research Council, September 1986.